10894 *Inorg. Chem.* **2010**, *49*, 10894–10901
DOI: 10.1021/ic1013076

Inorganic Chemistry
Article

Slow Relaxation of the Magnetization in Non-Linear Optical Active Layered Mixed Metal Oxalate Chains

Elena Cariati,*,† Renato Ugo,† Giuseppe Santoro,† Elisa Tordin,† Lorenzo Sorace,*,‡ Andrea Caneschi,‡ Angelo Sironi,§ Piero Macchi,∥ and Nicola Casati§,⊥

†*Dipartimento di Chimica Inorganica, Metallorganica e Analitica "Lamberto Malatesta" e UdR INSTM Università di Milano, via Venezian 21, 20133 Milano, Italy,* ‡*Dipartimento di Chimica "Ugo Schiff" e UdR INSTM Università di Firenze, Via della Lastruccia 3, 50019 Sesto Fiorentino (FI), Italy,* §*Dipartimento di Chimica Strutturale e Stereochmica Inorganica, Università di Milano, via Venezian 21, 20133 Milano, Italy,* ∥*Department of Chemistry and Biochemistry, University of Bern, Freiestrasse 3, CH3012 Bern, Switzerland, and* ⊥*Diamond Light Source Ltd., Harwell Science and Innovation Campus, Didcot, Oxfordshire OX11 0DE, U.K.*

Received June 30, 2010

New Co^{II} members of the family of multifunctional materials of general formula $[DAMS]_4[M_2Co(C_2O_4)_6]\cdot 2DAMBA\cdot 2H_2O$ (M^{III} = Rh, Fe, Cr; DAMBA = *para*-dimethylaminobenzaldehyde and $[DAMS^+]$ = *trans*-4-(4-dimethylaminostyryl)-1-methylpyridinium) have been isolated and characterized. Such new hybrid mixed metal oxalates are isostructural with the previously investigated containing Zn^{II}, Mn^{II}, and Ni^{II}. This allows to preserve the exceptional second harmonic generation (SHG) activity, due to both the large molecular quadratic hyperpolarizability of $[DAMS^+]$ and the efficiency of the crystalline network which organizes $[DAMS^+]$ into head-to-tail arranged J-type aggregates, and to further tune the magnetic properties. In particular, the magnetic data of the Rh^{III} derivative demonstrate that high spin octacoordinated Co^{II} centers behave very similarly to the hexacoordinated Co^{II} ones, being dominated by a large orbital contribution. The Cr^{III} derivative is characterized by ferromagnetic $Cr^{III}-Co^{II}$ interactions. Most relevantly, the Fe^{III} compound is characterized by a moderate antiferromagnetic interaction between Fe^{III} and Co^{II}, resulting in a ferrimagnetic like structure. Its low temperature dynamic magnetic properties were found to follow a thermally activated behavior ($\tau_0 = 8.6\times10^{-11}$ s and ΔE = 21.4 K) and make this a candidate for the second oxalate-based single chain magnet (SCM) reported up to date, a property which in this case is coupled to the second order non linear optical (NLO) ones.

Introduction

In the past years, hybrid inorganic−organic materials with interesting electrical, magnetic, emissive, and non-linear optical (NLO) properties have attracted the interest of the materials science community.[1−3] In particular, the addition of a novel degree of freedom to NLO systems, namely, the magnetic one, opens a yet largely unexplored research field. Although some magnetic materials displaying efficient second harmonic generation (SHG) have been reported,[4] hybrid inorganic−organic materials in which the magnetic properties can be easily and rationally tuned without affecting the SHG efficiency are still rare. In most multifunctional inorganic−organic hybrid materials the provider of the magnetic properties is the inorganic part, while the second-order NLO response more frequently originates from the organic counterpart. In these mixed systems changes of the inorganic framework often lead to severe structural changes of the whole crystal structure inducing nonobvious variations of the SHG efficiency of the hybrid material. However, in layered hybrid inorganic−organic crystalline materials structural distortions induced by changes of the magnetic ions into the inorganic layer can be easily absorbed without significantly altering the whole crystalline framework, making them

*To whom correspondence should be addressed. Phone: +39 0250314374 (E.C.), +39 0554573336 (L.S.). Fax: +39 0250314405 (E.C.), +39 0554573372 (L.S.). E-mail: elena.cariati@unimi.it (E.C.), lorenzo.sorace@unifi.it (L.S.).

(1) (a) Knutson, J. L.; Martin, D. J.; Mitzi, D. B. *Inorg. Chem.* **2005**, *44*, 4699. (b) Takahashi, Y.; Obara, R.; Nakagawa, K.; Nakano, M.; Tokita, J.; Inabe, T. *Chem. Mater.* **2007**, *19*, 6312. (c) Bi, W.; Leblanc, N.; Mercier, N.; Auban-Senzier, P.; Pasquier, C. *Chem. Mater.* **2009**, *21*, 4099.

(2) (a) Rabu, P.; Drillon, M. *Adv. Eng. Mater.* **2003**, *5*, 189. (b) Mahata, P.; Sen, D.; Natarajan, S. *Chem. Commun.* **2008**, 1278. (c) Delahaye, E.; Eyele-Mazui, S.; Bardeau, J. F.; Leuvrey, C.; Marger, L.; Rabu, P.; Rogez, G. *J. Mater. Chem.* **2009**, *19*, 6106. (d) Djerdj, I.; Cao, M.; Rocquefelte, X.; Černy, R.; Jagličić, Z.; Arčon, D.; Potočnik, A.; Gozzo, F.; Niederberger, M. *Chem. Mater.* **2009**, *21*, 3356.

(3) (a) Coe, B. J.; Curati, N. R. *Comments Inorg. Chem.* **2004**, *25*, 147. (b) Valore, A.; Colombo, A.; Dragonetti, C.; Righetto, S.; Roberto, D.; Ugo, R.; De Angelis, F.; Fantacci, S. *Chem. Commun.* **2010**, 2414. (c) Trujillo, A.; Fuentealba, M.; Carrillo, D.; Manzur, C.; Ledoux-Rak, I.; Hamon, J. R.; Saillard, J. Y. *Inorg. Chem.* **2010**, *49*, 2750.

(4) (a) Clément, R.; Lacroix, P. G.; O 'Hare, D.; Evans, J. *Adv. Mater.* **1994**, *6*, 794. (b) Bénard, S.; Yu, P.; Coradin, T.; Rivière, E.; Clément, R. *Adv. Mater.* **1997**, *9*, 12. (c) Bénard, S.; Yu, P.; Audière, P.; Rivière, E.; Clément, R.; Guilhem, J.; Tchertanov, L.; Nakatami, K. *J. Am. Chem. Soc.* **2000**, *122*, 9444. (d) Evans, J. S. O.; Bénard, S.; Yu, P.; Clément, R. *Chem. Mater.* **2001**, *13*, 3813.

Published on Web 11/10/2010

Scheme 1

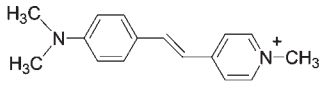

trans-4-(4-dimethylaminostyryl)-1-methylpyridinium

[DAMS$^+$]

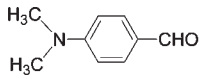

p-dimethylaminobenzaldehyde

[DAMBA]

particularly well suited for tuning in a rational way the magnetic properties without affecting the SHG efficiency. In this regard, we have recently reported the synthesis as well as the structural, magnetic, spectroscopic, and NLO characterization of a new promising family of magnetic and second-order NLO isostructural layered hybrid inorganic−organic materials of general formula $[M^{III}_2M^{II}(C_2O_4)_6]$-$[DAMS]_4[DAMBA]_2\cdot 2H_2O$ (where M^{III} = Rh, Fe, Cr; M^{II} = Mn, Zn, Ni; DAMBA = *p*-$N(CH_3)_2C_6H_4CHO$ and [DAMS$^+$] is the second order NLO chromophore *trans*-4-(4-dimethylaminostyryl)-1-methylpyridinium cation; see Scheme 1).[5]

This class of materials possesses some important structural features: it segregates layers of J-aggregated [DAMS$^+$] NLO chromophores and of mixed metal oxalate stripes of M^{III} and M^{II} cations which can be properly chosen to produce specific magnetic behaviors. The variety of magnetic properties which arises from different M^{III}/M^{II} pairs does not affect the very high SHG efficiency. In view of this tunability of the magnetic properties and of the particular structural arrangement, we extended our investigation to the Co^{II} members of this new class of hybrid mixed oxalates. The aim was to obtain a hybrid material with both high second order NLO properties and possibly Single Chain Magnet (SCM) ones. The latter are one-dimensional (1D) magnetic polymers whose magnetization relaxes slowly at low-temperatures and were the focus of intense research work in recent years,[6,7] since the first discovery of this peculiar behavior in a cobalt-organic radical system.[8] The presence between the inorganic layers of a large organic layer responsible for the second order NLO behavior makes this family of mixed M^{III}/M^{II} metal oxalates particularly suited to obtain monodimensional magnetic behavior, since the organic layer strongly reduces the interchain interaction. However, the 1D systems containing the Mn^{II} ion previously investigated[5a] were characterized by weak intrachain exchange interactions, leading to reduced correlation lengths among the spins and hampering any possibility of obtaining SCM behavior. More promising results were obtained with the Ni^{II} derivatives, with improved intrachain exchange interactions.[5b] However, also for the stripes including Ni^{II} centers, no sign of slow relaxation of the magnetization down to 2 K could be detected. This was attributed to the competing nearest-neighbor and next-nearest-neighbor interactions, giving rise to a magnetic state in which the Ni^{II} sublattice gives no neat magnetic contribution. In summary, these latter results confirmed that exchange coupling interactions could be obtained in this class of new hybrid materials while retaining the superior second order NLO properties; therefore, the preparation and characterization of Co^{II} derivatives was envisaged as an obvious extension. It is indeed well-known that, to obtain slow relaxation of the magnetization at low temperature, beyond a good isolation between adjacent magnetic chains, the second necessary property is a strong anisotropy of at least one magnetic center. In this respect both Co^{II} and Ln^{III} containing systems, with the large magnetic anisotropy imposed by these metal centers, are currently actively being investigated to obtain new SCM systems. Following this expectation recently a dysprosium-radical derivative[9] has been shown to behave as a SCM at low temperature while keeping the features of a second order NLO active material. It is worth noting that the possibility of obtaining oxalate-based SCMs, in spite of their relatively weak exchange interactions, has been recently reported by Coronado and co-workers.[10]

In the present study, we will report on the structural, second-order NLO, and magnetic properties of the Co^{II} derivatives of this new class of multifunctional hybrid mixed metal oxalates first investigated in our laboratories,[5] and in particular on the simultaneous occurrence, in one of them, of SCM-like behavior at low temperature still maintaining the high second order and NLO response.

Experimental Section

General Procedures and Materials. $K_3[M(C_2O_4)_3]\cdot nH_2O$ (M = Rh,[11] Cr, and Fe[12]) were prepared according to the literature. [DAMS]I and $Co(NO_3)_2\cdot 6H_2O$ were purchased from Sigma−Aldrich and used without further purification. All relevant phases were characterized by powder X-ray diffraction (XRPD) and $Fe^{III}_2Co^{II}$ by single crystal X-ray diffraction

(5) (a) Cariati, E.; Macchi, R.; Roberto, D.; Ugo, R.; Galli, S.; Casati, N.; Macchi, P.; Sironi, A.; Bogani, L.; Caneschi, A.; Gatteschi, D. *J. Am. Chem. Soc.* **2007**, *129*, 9410. (b) Cariati, E.; Macchi, R.; Tordin, E.; Ugo, R.; Bogani, L.; Caneschi, A.; Macchi, P.; Casati, N.; Sironi, A. *Inorg. Chim. Acta* **2008**, *361*, 4004.

(6) (a) Bogani, L.; Vindigni, A.; Sessoli, R.; Gatteschi, D. *J. Mater. Chem.* **2008**, *18*, 4750. (b) Brooker, S.; Kitchen, J. A. *Dalton Trans.* **2009**, 7331. (c) Miyasaka, H.; Julve, M.; Yamashita, M.; Clerac, R. *Inorg. Chem.* **2009**, *48*, 3420.

(7) (a) Bukharov, A. A.; Ovchinnikov, A. S.; Baranov, N. V.; Inoue, K. *Eur. Phys. J. B* **2009**, *70*, 369. (b) Vindigni, A.; Pini, M. G. *J. Phys.: Condens. Matter* **2009**, *21*, 236007. (c) Przybylak, S. W.; Tuna, F.; Teat, S. J.; Winpenny, R. E.P. *Chem. Commun.* **2008**, 1983. (d) Bernot, K.; Luzon, J.; Sessoli, R.; Vindigni, A.; Thion, J.; Richeter, S.; Leclercq, D.; Larionova, J.; van der Lee, A. *J. Am. Chem. Soc.* **2008**, *130*, 1619. (e) Ishii, N.; Okamura, Y.; Chiba, S.; Nogami, T.; Ishida, T. *J. Am. Chem. Soc.* **2008**, *130*, 24. (f) Bernot, K.; Bogani, L.; Caneschi, A.; Gatteschi, D.; Sessoli, R. *J. Am. Chem. Soc.* **2006**, *128*, 7947. (g) Toma, L. M.; Lescouezec, R.; Pasan, J.; Ruiz-Perez, C.; Vaissermann, J.; Cano, J.; Carrasco, R.; Wernsdorfer, W.; Lloret, F.; Julve, M. *J. Am. Chem. Soc.* **2006**, *128*, 4842. (h) Bogani, L.; Sangregorio, C.; Sessoli, R.; Gatteschi, D. *Angew. Chem., Int. Ed.* **2005**, *44*, 5817. (i) Bogani, L.; Caneschi, A.; Fedi, M.; Gatteschi, D.; Massi, M.; Novak, M. A.; Pini, M. G.; Rettori, A.; Sessoli, R.; Vindigni, A. *Phys. Rev. Lett.* **2004**, *92*, 207204. (j) Lescouezec, R.; Vaissermann, J.; Ruiz-Perez, C.; Lloret, F.; Carrasco, R.; Julve, M.; Verdaguer, M.; Dromzee, Y.; Gatteschi, D.; Wernsdorfer, W. *Angew. Chem., Int. Ed.* **2003**, *42*, 1483. (k) Clerac, R.; Miyasaka, H.; Yamashita, M.; Coulon, C. *J. Am. Chem. Soc.* **2002**, *124*, 12837.

(8) Caneschi, A.; Gatteschi, D.; Lalioti, N.; Sangregorio, C.; Sessoli, R.; Venturi, G.; Vindigni, A.; Rettori, A.; Pini, M. G.; Novak, M. A. *Angew. Chem., Int. Ed.* **2001**, *40*, 1760.

(9) Bogani, L.; Cavigli, L.; Bernot, K.; Sessoli, R.; Gurioli, M.; Gatteschi, D. *J. Mater. Chem.* **2006**, *16*, 2587.

(10) (a) Coronado, E.; Galan-Mascaros, J. R.; Marti-Gastaldo, C. *CrystEngComm* **2009**, *11*, 2143. (b) Coronado, E.; Galan-Mascaros, J. R.; Marti-Gastaldo, C. *J. Am. Chem. Soc.* **2008**, *130*, 14987.

(11) Werner, A.; Poupardin, J. *Ber. Dtsch. Chem. Ges.* **1914**, *47*, 1955.

(12) Bailar, J. C.; Jones, E. M. *Inorg. Synth.* **1939**, *1*, 35.

(XRD). Elemental analysis (C, H, N) were carried out in the Dipartimento di Chimica Inorganica, Metallorganica e Analitica "Lamberto Malatesta" of the University of Milano. M(II), M(III) analyses were performed in the Dipartimento di Chimica "U. Schiff", University of Florence, by using a Perkin-Elmer Optima 2000 inductively coupled plasma-optical emission spectrometer. Electronic absorption spectra were recorded on a Jasco V-530 spectrophotometer.

Preparation of Phases $\alpha_{MIII/CoII}$ (M = Cr, Fe, Rh). In a 100 mL two-necked flask [DAMS]I (183.2 mg, 0.50 mmol) was dissolved in 40 mL of H_2O/CH_3OH (1:1). The solution was heated at 60 °C, and 0.5 mmol $K_3[M(C_2O_4)_3]\cdot nH_2O$ (M = Rh, Fe, Cr), previously dissolved in 20 mL of H_2O/CH_3OH (1:1), were added. The heating was turned off, and $Co(NO_3)_2\cdot 6H_2O$ (145.5 mg, 0.5 mmol), dissolved in CH_3OH (2−3 mL), was added to the still hot solution. A brownish-black precipitate separated immediately as phase $\alpha_{MIII/CoII}$. After 1 h 30 min stirring at room temperature the solid was filtered, washed with a few drops of H_2O/CH_3OH (1:1), and dried under vacuum. Attempts to grow suitable single crystals for X-ray diffraction failed. Phases $\alpha_{MIII/CoII}$ were characterized by XRPD and found corresponding to $\alpha_{MIII/MII}$ (M^{III} = Rh, Cr, Fe; M^{II} = Zn, Mn, Ni).[13]

$[M_2Co(C_2O_4)_6][DAMS]_4[DAMBA]_2\cdot 2H_2O$ (M = Cr, Fe). In a 100 mL flask DAMBA (20.5 mg; 0.14 mmol) was added to the corresponding $\alpha_{CrIII/CoII}$ or $\alpha_{FeIII/CoII}$ phase (80.0 mg), prepared as above-reported, dissolved in 70 mL of H_2O/CH_3OH (1:1). The solution was heated under reflux for 1 h 30 min and then cooled at room temperature. On standing overnight, the formation of a dark compound with a metallic luster was observed. After filtration, the compound was dried under vacuum. Crystals of $Fe^{III}{}_2Co^{II}$ suitable for single crystal X-ray diffraction analysis were obtained by leaving the solution at room temperature for 3 days.

Anal. Calcd for $C_{94}H_{102}CoCr_2N_{10}O_{28}$ ($Cr^{III}{}_2Co^{II}$): C, 56.88; H, 5.14; N, 7.07; Co, 2.97; Cr, 5.24. Found: C, 57.06; H, 5.16; N, 7.18; Co, 3.05; Cr, 5.36%.

Anal. Calcd for $C_{94}H_{102}CoFe_2N_{10}O_{28}$ ($Fe^{III}{}_2Co^{II}$): C, 56.67; H, 5.13; N, 7.03; Co, 2.96; Fe, 5.61. Found: C, 56.54; H, 5.08; N, 7.10; Co, 3.06; Fe, 5.49%.

$[Rh_2Co(C_2O_4)_6][DAMS]_4[DAMBA]_2\cdot 2H_2O$. In a 100 mL flask DAMBA (80.0 mg; 0.55 mmol) was added to $\alpha_{RhIII/CoII}$ phase (80.0 mg), prepared as above-reported, dissolved in 70 mL of H_2O. The solution was heated under reflux for 1 h 30 min and then cooled at room temperature. On standing overnight, the formation of a dark compound with a metallic cluster was observed. After filtration, the compound was dried under vacuum. Crystals suitable for single crystal XRD analysis were obtained by leaving the solution at room temperature for 3 days.

Anal. Calcd for $C_{94}H_{102}CoN_{10}O_{28}Rh_2$ ($Rh^{III}{}_2Co^{II}$): C, 54.11; H, 4.89; N, 6.72; Co, 2.83; Rh, 9.87. Found: C, 54.13; H, 5.00; N, 6.85; Co, 2.91, Rh 9.69%.

Solid-State SHG by Kurtz−Perry Measurements.[14] The 1064 nm initial wavelength of a Nd:YAG pulsed laser beam was shifted to 1907 nm by stimulated scattering in a high-pressure hydrogen cell. A portion of this beam was directed on sample containing capillaries. The scattered radiation was collected by an elliptical mirror, filtered to select only the second-order contribution, and recollected with a Hamamatsu R5108 photomultiplier tube. SHG efficiency was evaluated by taking as reference the SHG signal of [DAMS][*p*-toluenesulfonate][15] or urea.

Single Crystal X-ray Diffraction Measurements. A crystal of $[Fe_2Co(C_2O_4)_6][DAMS]_4\cdot 2DAMBA\cdot 2H_2O$ was mounted on a glass fiber and collected on a Bruker SMART APEX 2 CCD area-detector diffractometer. Data collection was carried out in air at room temperature. Crystal data are reported in Table 1.

Table 1. Crystallographic Data for $[Fe_2Co(C_2O_4)_6][DAMS]_4\cdot 2DAMBA\cdot 2H_2O$[a]

compound empirical formula	$C_{94}H_{102}CoFe_2N_{10}O_{28}$
formula weight	1990.5
temperature	298 (2) K
wavelength	0.71073 Å
crystal system, space group	orthorhombic, *Fdd*2
unit cell dimensions	a = 39.364(3) Å
	b = 48.759(4) Å
	c = 9.487(8) Å
volume	18210(3) Å^3
Z, calculated density	8, 1.450 Mg/m^3
absorption coefficient	0.58 mm^{-1}
F(000)	8296
crystal size	0.25 × 0.05 × 0.02 mm
θ range for data collection	2.23 to 23.3°
reflections collected/unique	32216/6515
R(int)	0.21
R_σ	0.16
data/restraints/parameters	6515/1/379
goodness-of-fit on F^2	1.009
final R indices [$I > 2\sigma(I)$]	R1 = 0.0924, wR2 = 0.2127
R indices (all data)	R1 = 0.2095, wR2 = 0.2801

[a] $R_{int} = \sum|F_o^2 - F_{mean}^2|/\sum F_o^2$; $R_\sigma = \sum\sigma(F_o^2)/\sum F_o^2$; $R_1 = \sum||F_o| - |F_c||/\sum|F_o|$; $wR_2 = (\sum(F_o^2 - F_c^2)^2/\sum wF_o^4)^{1/2}$.

Graphite-monochromatized Mo−K_α (λ = 0.71073 Å) radiation was used with the generator working at 50 kV and 30 mA. Orientation matrix was initially obtained from least-squares refinement on about 300 reflections measured in three different ω regions, in the range $0 < \theta < 30°$; cell parameters were eventually optimized on the position, determined after integration, of all reflections above 10 $\sigma(I)$ level. 1080 frames, at 60 s per frame respectively, were collected with $\Delta\omega = 0.5°$. Sample−detector distance was set at 6 cm; an empirical absorption correction was applied (SADABS).[16]

The structure was refined starting from the known crystal structure of the Mn^{II} analogues[5a] (using SHELX97[17] within the WINGX[18] suite of programs). Anisotropic temperature factors were assigned to all non-hydrogenic atoms. Hydrogen atoms were riding on their carbon atoms, though water hydrogens were not located and included in our solutions.

XRPD Analysis. The powders of all phases analyzed were gently ground in an agate mortar and then cautiously deposited in the hollow of an aluminum holder equipped with a zero background plate with the aid of a glass slide. Diffraction data (Cu Kα, λ = 1.5418 Å) were collected on a vertical scan Philips PW1820 diffractometer with the generator operating at 40 kV and 40 mA. Intensities were measured in the range $5 < 2\theta < 35°$, typically with step scans 0.02° (10 s/step).

Magnetic Measurements. Direct current (DC) magnetic measurements were performed by using a Cryogenic S600 SQUID magnetometer operating between 2 and 300 K and with an applied field ranging from 0 to 6 T or with a QD MPMS working in the same range of temperature between 0 and 5 T. The latter instrument was also used to perform alternating current (AC) measurements at frequencies below 1 kHz in the temperature range 1.8−12 K. For higher frequencies (400−25000 Hz) and lower temperature (1.6−3.9 K) AC measurements have been performed using a home developed probe based on the Oxford Inst. MAGLAB platform.[19] All the samples were prepared by

(13) Interestingly the XRPD pattern for $\alpha_{CrIII/CoII}$ was consistently different to the others reported for "α"intermediate, although it showed comparable crystallinity and SHG efficiency.

(14) Kurtz, K.; Perry, T. T. *J. Appl. Phys.* **1968**, *39*, 3798.
(15) Marder, S. R.; Perry, J. W.; Yakymyshyn, C. P. *Chem. Mater.* **1994**, *6*, 1137.
(16) Sheldrick, G. M. *SADABS 2004/1*; University of Göttingen: Göttingen, Germany, 2004.
(17) Sheldrick, G. M. *SHELX97-Program for the refinement of Crystal Structure*; University of Göttingen: Göttingen, Germany, 1997.
(18) Farrugia, L. J. *J. Appl. Crystallogr.* **1999**, *32*, 837.
(19) Midollini, S.; Orlandini, A.; Rosa, P.; Sorace, L. *Inorg. Chem.* **2005**, *44*, 2060.

grinding freshly filtered crystals and then wrapping the powder in a Teflon tape. Measurements were repeated also by pressing the sample in a pellet to check for possible orientation effects. Magnetic susceptibilities were corrected for diamagnetism by using Pascal's constants. The diamagnetic contributions of the sample holder and the Teflon tape were independently measured and subtracted.

Computational Details

An Angular Overlap Model based program[20] has been used to calculate the energy levels pattern of the Co^{II} ion in different coordination environments. The anisotropic properties of the two lowest lying doublets were then fitted to an effective spin Hamiltonian using the Gerloch formula.[21] The polar coordinates of the ligand atoms derived from the X-ray structure were used to model the octacoordinated system, and the ligand field parameters of the two oxygen groups at different bond lengths were set as follows: Dq1 = 1200 cm^{-1}, Dq2 = 400 cm^{-1}, ζ = −426 cm^{-1}, B = 880 cm^{-1}, C = 3500.0 cm^{-1} e_π/e_σ = 0.2. For the sake of comparison, we also calculated the energy pattern and corresponding g values of an idealized octacoordinated system with the same polar coordinates and ligand atoms supposed at the same distances (i.e., with only one Dq parameters for all the eight ligand atoms). Finally, the energy pattern of a tetracoordinated system obtained by considering only the four ligands at shorter distance was calculated.

Results and Discussion

Synthesis, Spectroscopic, Second Order NLO, and Structural Characterization. As already reported, the best synthetic method to obtain compounds of the family of mixed oxalates of general formula $[M^{III}_2M^{II}(C_2O_4)_6]$-$[DAMS]_4[DAMBA]_2\cdot 2H_2O$ (where M^{III} = Rh, Fe, Cr; M^{II} = Mn, Zn, Ni; DAMBA = *p*-$N(CH_3)_2C_6H_4CHO$, $[DAMS^+]$ = *trans*-4-(4-dimethylaminostyryl)-1-methylpyridinium) consists in a two step procedure.[5] In the first step intermediated $\alpha_{MIII/MII}$ phases are obtained by mixing in water $K_3[M(C_2O_4)_3]\cdot nH_2O$ (M = Rh, Fe, Cr), M^{II} (M = Mn, Zn, Ni) salts and [DAMS]I. Despite the impossibility of isolating single crystals suitable for XRD characterization, $\alpha_{MIII/MII}$ phases have been found to be isomorphous by XRPD analysis, and characterized by a strong SHG of the same order of magnitude of [DAMS]-[*p*-toluenesulfonate] (i.e., 1000 times that of urea)[15] measured by the Kurtz−Perry method.[14] In the second step, $\alpha_{MIII/MII}$ phases are dissolved in H_2O, added with DAMBA, and heated under reflux to produce compounds of this new family of hybrid mixed oxalates.

$[M^{III}_2Co^{II}(C_2O_4)_6][DAMS]_4[DAMBA]_2\cdot 2H_2O$ (where M = Cr, Fe, Rh; hereafter indicated as $Cr^{III}_2Co^{II}$, $Fe^{III}_2Co^{II}$, $Rh^{III}_2Co^{II}$, respectively, or collectively as $M^{III}_2Co^{II}$) were prepared by applying a slightly modified version of this two step method (see the Experimental Section). By the Kurtz−Perry method,[14] working with a non-resonant wavelength of 1907 nm, all $M^{III}_2Co^{II}$ hybrid crystalline materials were found to be characterized by the same very high SHG (same order of magnitude of [DAMS]-[*p*-toluenesulfonate] working at the same incident wavelength[15]).

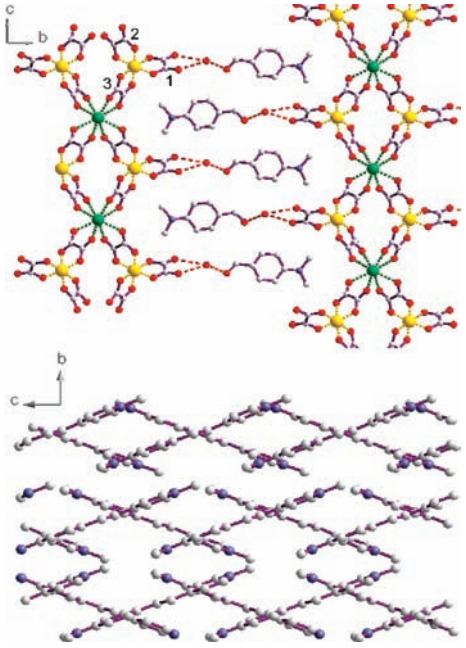

Figure 1. View, along the crystallographic *a* axis, of the inorganic/organic layer (top), and of the relative organization of the $[DAMS^+]$ molecules (bottom). Gray, Carbon atoms; Red, oxygen atoms; Blue, nitrogen atoms; Green, M^{II} sites; Yellow, M^{III} sites. Hydrogen atoms are not shown, for the sake of clarity. The three independent oxalates (1, 2, and 3) are indicated, as well as the stronger hydrogen bonding connections, that involve the "lateral" oxalate ligands (having two free oxygens), the DAMBA molecules, and the water molecules. Weaker C−H---O connections are not represented. Two metal-oxalate stripes, elongated along the direction of the *c* crystallographic axis, can be recognized.

As reported for all the compounds of this family of mixed hybrid oxalates investigated so far,[5] solid-state electronic absorption spectra of $M^{III}_2Co^{II}$ compounds show the superposition of two bands: a broad and strong band centered at 464 nm and a strong, narrow band at 568 nm. This latter has been identified as the fingerprint of J aggregation of the $[DAMS^+]$ chromophore.[5] In acetonitrile solution $M^{III}_2Co^{II}$ compounds all show an absorption spectrum identical to that of [DAMS]I, with an absorption band at 471 nm because of the disruption of the ordered J aggregates by dissolution in a polar organic solvent.

$M^{III}_2Co^{II}$ compounds have been found by XRPD to be isomorphous (see Supporting Information, Figure S1) to the previously structurally characterized congeners of this family (M^{III} = Cr, Fe, Rh; M^{II} = Mn, Ni, Zn) crystallizing in the polar acentric *Fdd*2 space group.[5] The crystalline structure of the $Fe^{III}_2Co^{II}$ compound was solved by XRD analysis of suitable single crystals (see the Experimental Section). The large asymmetric unit contains two independent $[DAMS^+]$ ions, one DAMBA, one water molecule, three oxalate anions, one Fe^{III} atom in a general position, and one Co^{II} in a 2-fold special position.

Differently from other mixed layered metal-oxalates of $[DAMS^+]$,[4] all these hybrid materials are characterized by layers of mixed metal oxalates based on an organic−inorganic 2D framework, rather than a purely inorganic one. The inorganic part of this layer is composed by the metal ions and the coordinated oxalates, forming infinite stripes (∼14 Å large) (see Figure 1), elongated along the *c* axis. The M^{II} cations are bound to four oxalate groups in a distorted square anti prismatic coordination environment

(20) Bencini, A.; Ciofini, I.; Uytterhoeven, M. *Inorg. Chim. Acta* **1998**, *274*, 90.
(21) Gerloch, M.; McMeeking, R. F. *J. Chem. Soc., Dalton Trans.* **1975**, 2443.

Table 2. M^{II}−O Distances in $[Fe^{III}_2M^{II}(C_2O_4)_6][DAMS]_4\cdot 2DAMBA\cdot 2H_2O$ Compounds Structurally Characterized by Single Crystal X-ray Diffraction Analysis

	M^{III} = Fe		
	M^{II} = Mn[5a]	M^{II} = Ni[5b]	M^{II} = Co
bridging oxalate 2	2.592(3)	2.589(6)	2.56(1)
	2.265(3)	2.416(6)	2.39(1)
bridging oxalate 3	2.472(3)	2.530(6)	2.52(1)
	2.295(3)	2.451(6)	2.43(1)

while the M^{III} cations are octahedrally coordinated by three oxalate groups. One of these latter stretches out from the stripe, whereas the other two oxalates bridge M^{III} and M^{II}, forming a peculiar -M^{II}-(M^{III})$_2$-M^{II}-(M^{III})$_2$-M^{II}- 1D quite unusual motif. Details about the metal to oxygen bond length of this rather uncommon, at least for Co^{II} and Ni^{II}, cubic antiprismatic coordination are reported in Table 2; notably the Co environment is closer to that of Ni rather than that of Mn in the corresponding $Fe^{III}_2M^{II}$ compounds.

As already reported for this family of mixed metal oxalates,[5] each pair of stripes is spaced by ∼10 Å and shifted by 1/2 along *c*, producing a mismatch of the lateral branches, as shown in Figure 1 (top). The volume between the stripes is used to accommodate bridges formed by DAMBA and water molecules. Such a two-dimensional (2D) layer is held together by medium/strong O−H---O hydrogen bonds (Oxalate---water---DAMBA, water acting as HB donor with O---O distances of about 2.9 Å) and weaker C−H---O hydrogen bonds (DAMBA---oxalate, DAMBA being the donor). This entanglement produces a compact but flexible mixed organic/inorganic layer parallel to (100), where DAMBA acts as a fundamental building block, not just as a spacer. The mixed inorganic/organic layers are negatively charged, with a surface density of charge of about 0.008 e/Å^2 (a charge of −4 spread over a surface of about 462 Å^2, corresponding to the (1 0 0) plane). This perfectly fits the charge/area ratio obtained by a layer of tightly packed, as J aggregates, [$DAMS^+$] ions. Hence, the overall structure contains alternating negatively and positively charged layers, all parallel to the [100] plane and stacking one on top of another along the *a* axis (Figure 2, bottom).

The origin of the strong SHG is related to the arrangement of [$DAMS^+$] chromophores inside the crystalline framework which has been fully discussed in our first report[5a] on this new class of hybrid M^{II}/M^{III} mixed oxalates.

Magnetic Properties

$[Rh^{III}_2Co^{II}(C_2O_4)_6][DAMS]_4[DAMBA]_2\cdot 2H_2O$. The peculiar magnetic behavior introduced by Co^{II} centers, which are well-known not to follow the Curie behavior,[22] was first investigated by studying the $M^{III}_2Co^{II}$ compound containing the diamagnetic Rh^{III} center. In general the introduction of Rh^{III} centers is expected to produce weak magnetic interactions inside the chain so that an experimental determination of the effects on the magnetic properties of $Rh^{III}_2Co^{II}$ could be attributable mainly to uncoupled Co^{II} centers. This is in itself an interesting output of this investigation, since the octacoordinated geometry is very rare in Co^{II} compounds[23] and no report on the magnetic behavior of the Co^{II} ion in this environment has, to the best of our knowledge, ever been reported. The χT versus T value (Figure 3) measured at room temperature (3.1 emu K mol^{-1}) is much higher than that for a spin-only value for $S = 3/2$, and indicates the persistence of a substantial unquenched orbital contribution in the square antiprismatic coordination, similar to what is usually reported for pseudo-octahedral Co^{II} coordination.[24] The decrease of χT observed on lowering temperature down to 100 K should be attributed for the same reason to depopulation effects of the levels arising from the splitting of the ground multiplet, since antiferromagnetic exchange interactions among Co^{II} ions, which are far apart from each other (15.8 Å) have to be excluded. This latter point is confirmed by the magnetization curve as a function of field, which tends to saturate at a value in agreement with an effective $S = 1/2$ and an average g value $g_{ave} = 4.3$ ($M = 2.1\,\mu_B$ at 6 T and 2 K, inset of Figure 3). This behavior resembles more that of the $Rh^{III}_2Mn^{II}$ compound, for which no interaction between the Mn^{II} centers were reported,[5a] than to that of the $Rh^{III}_2Ni^{II}$ compound, for which significant antiferromagnetic interactions were postulated.[5b] Furthermore, these results suggest that the magnetic behavior of this kind of octacoordinated Co^{II}, characterized by two largely

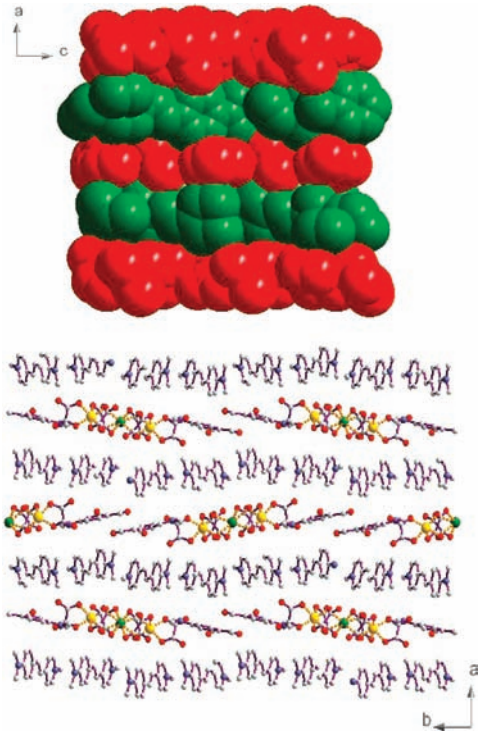

Figure 2. (Top) View, along the crystallographic *b* axis, of the layered structure formed by the [$DAMS^+$] layers and the inorganic/organic layers. The layers are alternatively charged with positive and negative charges. (Bottom) View of the layered crystal structure along the crystallographic *c* axis, showing the packing of two layers and the disposition of the oxalate-based chains in the structure. Hydrogen atoms are omitted for clarity.

(22) (a) Lloret, F.; Julve, M.; Cano, J.; Ruiz-García, R.; Pardo, E. *Inorg. Chim. Acta* **2008**, *361*, 3432. (b) Bencini, A.; Beni, A.; Costantino, F.; Dei, A.; Gatteschi, D.; Sorace, L. *Dalton Trans.* **2006**, 722.

(23) (a) Tsohos, A.; Dionyssopoulou, S.; Raptopoulou, C. P.; Terzis, A.; Bakalbassis, E. G.; Perlepes, S. P. *Angew. Chem., Int. Ed.* **1999**, *38*, 983. (b) Bergman, J. G.; Cotton, F. A. *Inorg. Chem.* **1966**, *5*, 1208. (c) Koch, W. O.; Kaiser, J. T.; Krüger, H.-J. *Chem. Commun.* **1997**, 2237.

(24) (a) Kahn, O. *Molecular Magnetism*; Wiley-VCH: Weinheim, 1993; (b) Carlin, R. L. *Magnetochemistry*; Springer-Verlag: West Berlin, Germany, 1986.

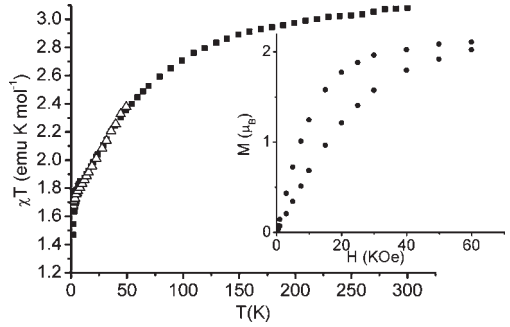

Figure 3. Temperature dependence of the χT product at 1 KOe (empty triangles) and 10 KOe (full squares) for $Rh^{III}{}_2Co^{II}$. In the inset the field dependent magnetization at 2 K (upper curve) and 4.5 K (lower curve) is reported.

different bond lengths resembles more that of octahedral Co^{II} (with largely unquenched orbital contribution) than that of tetrahedral Co^{II}, characterized by an orbitally singlet ground state.[24] To rationalize the observed properties we performed sample calculations on the basis of the Angular Overlap Model. Even if it is well-known that the anisotropic magnetic properties of Co^{II} are dramatically affected by small variation of low-symmetry ligand field components,[25] the results provided qualitative indication that the observed experimental behavior follows theoretical expectations. Indeed, for both tetracoordinated and octacoordinated Co^{II} centers with ligands at the same distance, calculations provide an estimate of the quartet ground state splitting of about 15 cm^{-1}, whereas for the octacoordinated systems characterized by four long coordination bonds the separation between the two ground doublets easily exceeds 50 cm^{-1}, closer to the result expected for of an hexacoordinated pseudo-octahedral system.[22] The same calculation also provide an estimate of the g values, suggesting that the ground doublet in $Rh^{III}{}_2Co^{II}$ is actually characterized by a quite strong Ising character, with $g_{x,y}$ about ≈ 1.6 and $g_z \approx 7.1$.

$[Cr^{III}{}_2Co^{II}(C_2O_4)_6][DAMS]_4[DAMBA]_2 \cdot 2H_2O$. The χT versus T value for $Cr^{III}{}_2Co^{II}$ derivative at room temperature (6.71 emu K mol-1) agrees quite well with the sum of the values of χT found for $Rh^{III}{}_2Co^{II}$ (3.1 emu K mol-1, see above) and $Cr^{III}{}_2Zn^{II}$ compounds (3.68 emu K mol^{-1}[5a]), suggesting the weakness of the magnetic interaction between adjacent paramagnetic centers such as Co^{II} and Cr^{III}, whose effects are not observable at this temperature. In accordance with this the χT curve (Figure 4) slowly decreases on cooling down to 200 K, in a way parallel with the decrease observed for the $Rh^{III}{}_2Co^{II}$ derivative. The decrease of χT should thus be attributed to single ion effects of Co^{II} ions, at least down to 200 K, while exchange coupling interactions are not effective in this temperature range. At lower temperatures, the plot of $(\chi T_{Cr2Co} - \chi T_{Rh2Co})$ versus T, which steadily increases with temperature, clearly testifies to the presence of ferromagnetic interactions,[26] which results in a χT versus T curve passing through a quite sharp maximum at 4 K (7.9 emu K mol^{-1}).

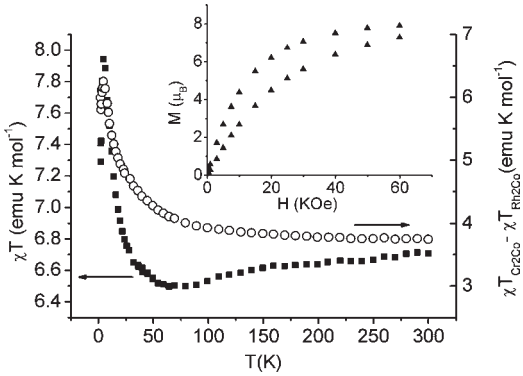

Figure 4. Temperature dependence of χT product for $Cr^{III}{}_2Co^{II}$ (left scale, full squares) and of $(\chi T_{Cr2Co} - \chi T_{Rh2Co})$ (right scale, empty circles). In the inset the field dependent magnetization at 2 K (upper curve) and 4.5 K (lower curve) for $Cr^{III}{}_2Co^{II}$ is reported.

The achievement of a ferromagnetic behavior of the Cr^{III}/Co^{II} chain is confirmed by the low temperature field dependent magnetization curves (inset of Figure 4), which attains a saturation value of 8 μ_B, in agreement with what is expected for a full "spin-up" configuration on the basis of the saturation values observed for $Cr^{III}{}_2Zn^{II}$[5a] and $Rh^{III}{}_2Co^{II}$ derivatives. The presence of a ferromagnetic interaction between Cr^{III} and Co^{II} centers at low temperatures is in agreement with what is reported for simple dinuclear and trinuclear cluster.[24]

It is, however, to be noticed that both the relatively low maximum value of χT and the shape of the M versus H curve, attaining saturation only at quite high fields, points to exchange interactions weaker than those reported for other $Cr^{III}-Co^{II}$ mixed oxalates.[27] This behavior can also be due to the competing effects of weak antiferromagnetic interactions between Cr^{III} ions, which were visible below 10 K in the $Cr^{III}{}_2Zn^{II}$ derivative.[5a] The relative weakness of the exchange coupling interaction, coupled to the good isolation provided by the organic layer, responsible for the second order NLO activity, results in the absence of both magnetic long-range order and single-chain magnet behavior, confirmed by the absence of any imaginary components (χ'') in the AC magnetic susceptibility.

$[Fe^{III}{}_2Co^{II}(C_2O_4)_6][DAMS]_4[DAMBA]_2 \cdot 2H_2O$. At room temperature the experimental value of χT (9.8 emu K mol^{-1}) of $Fe^{III}{}_2Co^{II}$ is lower than that expected assuming the three spins to be uncoupled, and considering the experimental values observed for $Rh^{III}{}_2Co^{II}$ and $Fe^{III}{}_2Zn^{II}$.[5a] This suggests the presence of sizable antiferromagnetic interactions, already visible at this temperature, as confirmed by the marked decrease of χT by lowering the temperature (Figure 5). This behavior can not be attributed to simple ligand field effects of Co^{II} centers, since the corresponding, isostructural, $Rh^{III}{}_2Co^{II}$ derivative shows a less marked temperature dependence of χT in the same range of temperatures. On further lowering the temperature χT passes through a minimum at 30 K (8.3 emu K mol^{-1}) and then starts to increase, a behavior reminiscent of a ferrimagnetic like structure, which indicates that antiferromagnetic interactions result in a non compensation of the spins, obviously suggesting that they

(25) Banci, L.; Bencini, A.; Benelli, C.; Gatteschi, D.; Zanchini, C. *Struct. Bonding* (*Berlin*) **1982**, *52*, 37.

(26) (a) Costes, J. P.; Dahan, F.; Dupuis, A.; Laurent, J. P. *Chem.—Eur. J.* **1998**, *4*, 1616. (b) Kahn, M. L.; Sutter, J.-P.; Golhen, S.; Guionneau, P.; Ouahab, L.; Kahn, O.; Chasseau, D. *J. Am. Chem. Soc.* **2000**, *122*, 3413–3421. (c) Caneschi, A.; Dei, A.; Gatteschi, D.; Poussereau, S.; Sorace, L. *Dalton Trans.* **2004**, 1048.

(27) (a) Ohba, M.; Tamaki, H.; Matsumoto, N.; Okawa, H. *Inorg. Chem.* **1993**, *32*, 5385. (b) Sun, Y.-Q.; Zhang, J.; Yang, G.-Y. *Dalton Trans.* **2006**, 1685.

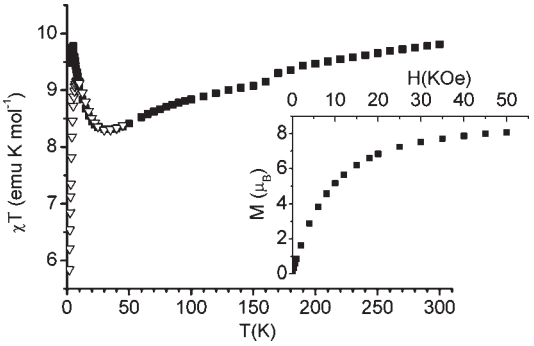

Figure 5. Temperature dependence of χT product at 1 KOe (full squares) and 10 KOe (empty triangles) for $Fe^{III}_2Co^{II}$. In the inset the field dependent magnetization at 2 K is reported.

are active between Fe^{III} and Co^{II} ions. On further lowering the temperature a maximum in χT, which is field dependent because of saturation effects, is observed (9.8 emu K mol^{-1} at 4.2 K for H ≤ 1 KOe, including AC measurements). The antiparallel orientation of the spin on Co^{II} and Fe^{III} sub lattices because of the dominating antiferromagnetic interactions is confirmed by the field dependent magnetization curve recorded at 2 K (inset of Figure 5), which saturates at about 8 μ_B, corresponding to the experimentally determined one for $M_{sat}(Fe^{III}_2Zn^{II}) - M_{sat}(Rh^{III}_2Co^{II})$. As a whole the observed behavior strongly resembles that observed for the $Fe^{III}_2Mn^{II}$ derivative[5a] and agrees with expectations of dominant antiferromagnetic interactions between Co^{II} and Fe^{III} mediated by oxalate bridges.[28]

The AC susceptibility measured at zero field rules out any long-range order: indeed, the imaginary contribution, which shows up below 4 K, is frequency dependent and should thus be attributed to dynamic effects (Figure 6). The analysis of the frequency dependence of χ'' maximum by the Arrhenius law, assuming that at the temperature of the maximum $\tau = (2\pi\nu)^{-1}$, yields as best fit values ($R^2 = 0.9681$) $\tau_0 = (8.6 \pm 0.5)\ 10^{-11}$ s and $\Delta E = 21.4 \pm 2$ K (inset of Figure 6). The physically reasonable values of τ_0 and ΔE, even if obtained in a somewhat restricted range of frequencies, rule out the possibility that the system is a spin glass and suggest that $Fe^{III}_2Co^{II}$ is behaving as a SCM at low temperature. It is, however, to be noted that the ratio between real (χ') and imaginary (χ'') components of the susceptibility is very large (see Supporting Information, Figure S2 for frequency dependent χ' data), suggesting either a broad distribution of relaxation times, which would also explain the broadness of the observed maxima in χ'' (Figure 6), or that only a fraction of the chains is showing slow relaxation of the magnetization.[29] This may also explain the somehow small value of the barrier ΔE to the reversal of the magnetization, compared to the expectations based on static magnetic measurements. Indeed, in a SCM this parameter is related to the strength of the exchange

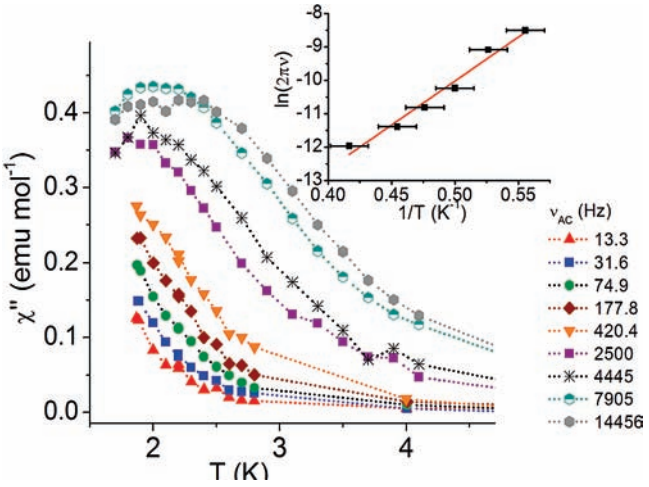

Figure 6. Temperature dependence of the out-of phase magnetic susceptibility at different frequencies (5−15000 Hz). In the inset, the corresponding Arrhenius plot with best fit line is reported.

interaction by the relation $\Delta E = 4J/kT$.[30] Thus, the relatively small ΔE value obtained here would point out a relatively weak magnetic interaction (ca. 5 K), in contrast with the χT versus T data, indicating sizable exchange magnetic interactions are active between Fe^{III} and Co^{II} centers even at room temperature.

Conclusions

The results obtained in this study confirm that substitution of either M^{II} or M^{III} metal centers in this new class of multifunctional hybrid mixed metal oxalates based on the second-order NLO chromophore [$DAMS^+$][5] does not alter the layered structure of these systems. In such crystalline network, hydrogen bonds involving DAMBA and water molecules play a major role in stabilizing inorganic chains of metal oxalates and allow an efficient control of the segregation of layers of [$DAMS^+$] chromophores self-organized in a head-to-tail disposition, forming NLO efficient J aggregates. This has the very important consequence of maintaining a strong SHG efficiency, which is provided by the organic layer, irrespectively of the metal ions employed.

A tuning of the magnetic properties of these mixed metal oxalates by suitable substitution of metal ion centers was then systematically pursued. In particular, previous studies[5b] had shown that the substitution of Mn^{II} centers by Ni^{II} may lead to largely different intrachain exchange interactions while maintaining the superior second order NLO properties. It was then obvious to extend our investigation to Co^{II} based systems, to analyze the effect of an expected largely anisotropic metal ions on the magnetic properties of these systems. A summary in terms of the nature of intrachain exchange magnetic interactions is reported in Table 3, where previously reported data on Mn^{II}[5a] and Ni^{II}[5b] based systems are also collected.

The first point to be noted concerns the $Rh^{III}_2Co^{II}$ compound, whose magnetic data show that high spin octacoordinated Co^{II} centers behave similarly to the hexacoordinated Co^{II} ones, being dominated by a large orbital contribution. Moreover, data in Table 3 evidence that virtually no exchange coupling interactions between Co^{II} centers is observed in this case, in similarity with the $Rh^{III}_2Mn^{II}$

(28) Coronado, E.; Galan-Mascaros, J. R.; Gimenez-Saiz, C.; Gomez-Garcia, C. J.; Ruiz-Perez, C. *Eur. J. Inorg. Chem.* **2003**, 2290.
(29) Langley, S.; Helliwell, M.; Sessoli, R.; Teat, S. J.; Winpenny, R. E. P. *Dalton Trans.* **2009**, 3102.
(30) Caneschi, A.; Gatteschi, D.; Lalioti, N.; Sangregorio, C.; Sessoli, R.; Venturi, G.; Vindigni, A.; Rettori, A.; Pini, M. G.; Novak, M. A. *Europhys. Lett.* **2002**, *58*, 771.

Table 3. Summary of the Nature of the Exchange Coupling Interactions between Metal Ions of the Chains in the Different Compounds of Mixed Metal Oxalates with Strong Second Order NLO Activity Reported up to Now

M^{III}	Ni^{II}	Mn^{II}	Co^{II}
Rh	antiferromagnetic (Ni−Ni)[5b]	negligible (Mn−Mn)[5a]	negligible (Co−Co)[this work]
Cr	ferromagnetic (Ni−Cr)[5b]	weakly ferromagnetic(Mn−Cr)[5a]	ferrromagnetic (Co−Cr)[this work]
Fe	ferromagnetic (Ni−Fe)[5b]	antiferromagnetic[5a]	antiferromagnetic[this work]

compound and at variance with the $Rh^{III}{}_2Ni^{II}$ one. The analysis of the magnetic behavior of the $Cr^{III}{}_2Co^{II}$ compound points out that this system is characterized, as already observed for the corresponding Mn^{II}[5a] and Ni^{II}[5b] ones, by ferromagnetic $M^{III}-M^{II}$ interactions. The most relevant result obtained in the present investigation concerns the $Fe^{III}{}_2Co^{II}$ compound, characterized by a moderate antiferromagnetic interaction between Fe^{III} and Co^{II}, resulting in a ferrimagnetic like structure. Its low temperature dynamic magnetic properties make this compound a candidate as the second oxalate-based SCM reported up to date, a property which in this case is coupled to the strong second order NLO activity. Our observation confirms the fundamental role of Co^{II} centers in giving rise to a 1D system with SCM behavior. As a further extension of this work we are currently planning the introduction of the Mn^{III} ion which is well-known to provide strong Ising-type anisotropy,[31] an important feature to obtain SCM behavior at a higher temperature.[7d,j,k]

Acknowledgment. P.M. acknowledges the Swiss National Science Foundation for financial support (project number 200021_125313). The financial support of Italian MIUR through FIRB RBNE033KMA and PRIN 2008 2008FZK5AC is gratefully acknowledged. We also thank the Fondazione CARIPLO (2005: Nuovi materiali con nanoorganizzazione di cromofori in sistemi HostGuest o su scaffold inorganico per dispositivi fotoluminescenti o optoelettronici; 2006: Materiali nanostrutturati autoassemblati: una strategia per il controllo delle proprietà elettroottiche).

Supporting Information Available: XRPD comparison of $Fe^{III}{}_2Co^{II}$ and $Rh^{III}{}_2Co^{II}$. Plot of χ' versus T at various frequencies. This material is available free of charge via the Internet at http://pubs.acs.org.

(31) Gatteschi, D.; Sorace, L. *J. Solid State Chem.* **2001**, *159*, 253.